

Mesoscopic transport in ultrathin films of $\text{La}_{0.67}\text{Ca}_{0.33}\text{MnO}_3$

C. Beekman, J. Zaanen and J. Aarts¹

¹*Kamerlingh Onnes Laboratorium, Leiden University, The Netherlands**

We investigate the electrical transport in mesoscopic structures of $\text{La}_{0.67}\text{Ca}_{0.33}\text{MnO}_3$ in the regime of the metal-insulator transition by fabricating microbridges from strained and unstrained thin films. We measure current-voltage characteristics as function of temperature and in high magnetic fields and with varying film thickness. For strained films, in warming from the metallic to the insulating state, we find non-linear effects in the steep part of the transition characterized by a differential resistance with a strong peak around zero applied current, and saturating at higher currents after resistance drops up to 60 %. We propose that this nonlinear behavior is associated with melting of the insulating state by injecting charge carriers, signalling the occurrence of an intervening phase which involves the formation of short range polaron correlations.

Doped manganites are strongly correlated electron systems which show a large variety in physical properties. The material $\text{La}_{0.67}\text{Ca}_{0.33}\text{MnO}_3$ (LCMO) for instance shows a transition from a paramagnetic insulator to a ferromagnetic metal around $T_{MI} = 250$ K and the well known colossal magnetoresistance (CMR) effect. The physics is mainly determined by competing interactions: trapping of the electrons in Jahn-Teller (JT) distortions (polarons) and the itinerancy of the electrons in the Double-Exchange mechanism [1] when spins become polarized. This competition signals that only small free energy differences exist between a variety of different possible phases of the system. As a result the phase of the material can be tuned easily by various external perturbations, such as magnetic and electric fields, strain and disorder. For instance, the application of strain amplifies the JT splitting of the e_g levels and makes the distortions more static in nature. This has an inhibiting effect on band formation, which leads to reduction of T_{MI} in manganite thin films compared to the bulk value [2, 3]. Furthermore, the susceptibility of the M-I transition to disorder (doping disorder, oxygen nonstoichiometry, defects from strain relaxation, twinning, and grain boundaries) can lead to the coexistence of the metallic and insulating phases on a variety of length scales [4, 5]. Electrical transport in these correlated electron systems is therefore a complex phenomenon, which has however hardly been probed on small length scales. Here we address such transport in the mesoscopic regime, by investigating microbridges made in LCMO thin films, grown in a strained or unstrained state on SrTiO_3 (STO) or NdGaO_3 (NGO) substrates. In the strained films we do find strongly nonlinear transport behavior in the CMR regime near the metal-insulator transition, characterized by increased conductance at higher current. We attribute these effects to the intrinsic physics of the insulating state in terms of the formation of an intervening glassy polaron state when going from the correlated metal to the polaronic insulator.

We have grown LCMO thin films with varying thicknesses between 7 - 20 nm on STO and NGO substrates, by DC-sputtering in an oxygen atmosphere of 3 mbar and

at a growth temperature of 840°C. The STO induces a tensile strain in the LCMO film due to the lattice mismatch of -0.6 %, the NGO is (almost) lattice matched. After growth, x-ray measurements were performed to check the thickness of the films. Furthermore, Electron Energy Loss Spectroscopy (EELS) was used to characterize the elemental composition and Mn valence state of the samples [6]. We find that our films have compositions close to that of the sputtering target and correct oxygen stoichiometry. The films were patterned using electron-beam lithography and conventional Ar-etching followed by an oxygen plasma etch to restore the insulating properties of the substrate [7]. The mesoscopic LCMO structure has a four-point configuration with dimensions of 5 μm (width) by 20 - 30 μm (length between voltage contacts), as shown in Fig.1a. Macroscopic Au/MoGe contacts were fabricated in a second e-beam step. We measured I - V curves as function of temperature and in high magnetic fields using a Physical Properties Measurement System (Quantum Design) for temperature control ($T = 20 - 300$ K) and for magnetic field control ($H_a = 0 - 9$ T), but with external current sources and voltmeters.

I - V characteristics, measured by varying the current, were obtained across the temperature range of 20 - 300 K in order to obtain the differential resistance. All microbridges were also measured in a magnetic field of 5 T to investigate the magnetoresistance (MR) effect. Our main findings are shown in Fig.1b. It shows the resistance vs. temperature ($R(T)$) of a microbridge on STO, measured at currents of 100 nA (current density $J = 2 \times 10^6$ A/m²) and 2 μA ($J = 4 \times 10^7$ A/m²). As can be seen in the inset, where $R(T)$ is plotted logarithmically, both sets of data show a clear M-I transition typical for strained LCMO thin films with $T_{MI} = 130$ K (peak temperature) and a resistance drop of three orders of magnitude. The main panel of Fig.1b shows $R(T)$ on a linear scale. The higher current density results in a reduction of resistance just below T_{MI} , which produces a shift in the upper part of the transition of 5 to 10 K. Also shown is the difference between the two curves, which peaks between 105 K and 110 K. If we define a current-induced resistance called

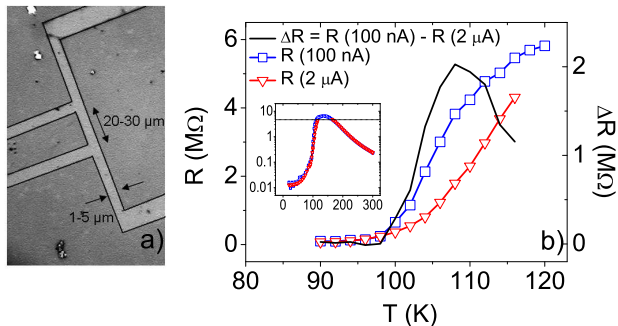


FIG. 1: (color on-line) a) electron microscopy picture of a typical microbridge. The width of the bridge is $5 \mu\text{m}$. b) $R(T)$ between $T = 90$ and 120 K at two different current densities ($J = 2 \times 10^6$ A/m 2 (squares) and $J = 4 \times 10^7$ A/m 2 (triangles)) for the 10 nm thick microbridge on STO (left axis). (right axis and solid line) the difference between the two curves, $\Delta R = R(100\text{nA}) - R(2\mu\text{A})$. Inset: $R(T)$ between $T = 20$ and 300 K for both current densities on a logarithmic scale. The dashed line indicates the measurement limit for the high current density measurement. The absence of resistance values above this limit is due to saturation of the nanovoltmeter.

Electroresistance ($\text{ER}(\%) = \frac{R_{\text{high}} - R_{\text{low}}}{R_{\text{low}}} \times 100\%$), then we observe a maximum ER effect up to 60 % for the 10 nm microbridge.

The measured I - V curves are linear for microbridges on NGO and linear for most temperatures in the case of STO. However, for microbridges on STO we find non-linear behavior in the steep part of the transition which corresponds to the behavior shown in Fig.1. Typical non-linear behavior is shown in Fig.2. The left panel shows the differential resistance for the 10 nm microbridge at four different temperatures in 0 T as function of applied current density (bottom axis) and also as function of the measured potential difference (V_m) between the voltage contacts (top axis). At low temperature all I - V curves are linear up to $J = 8 \times 10^7$ A/m 2 ($I = 4 \mu\text{A}$). Upon warming into the transition the nonlinear behavior starts to occur just below $T = 96$ K and appears to continue until T_{MI} . For all microbridges the differential resistance is largest at zero bias and drops with increasing applied current density. The full width of the peak appears to increase by more than an order of magnitude from about 2×10^6 A/m 2 (0.2 V) at $T = 96$ K up to 4×10^7 A/m 2 (8 V) at $T = 110$ K. However, due to the voltage limit of the nanovoltmeter, it is difficult to observe any nonlinear behavior between 110 K - 170 K. Above this temperature range all I - V curves are linear. From the right panel it is clear that application of a high magnetic field leads to a reduction in the differential resistance and to complete disappearance of the nonlinearities in the I - V curves; they are linear across the entire temperature range. To compare the differential resistance behavior of different microbridges we show ($\frac{dV}{dI}$, Fig.3), normalized

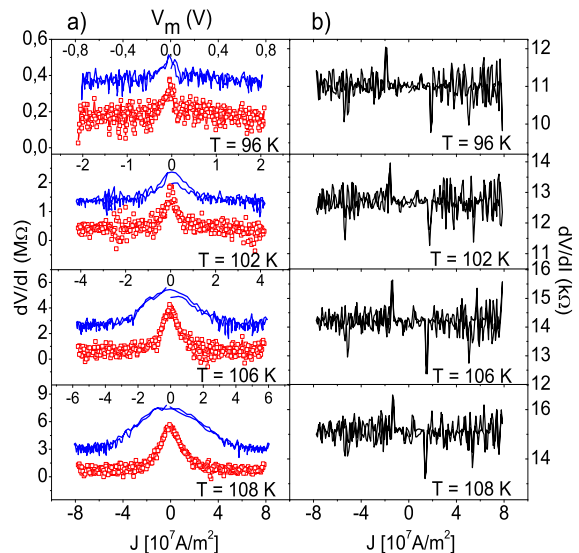


FIG. 2: (color on-line) The numerical derivatives of the I - V curves for the 10 nm thick microbridge on STO at four different temperatures of which the $R(T)$ behavior is shown in Fig. 1. a) Measured in 0 T. Bottom axis shows current density, J (symbols) and top axis indicates the measured potential difference (V_m) between the voltage contacts (solid line). b) Measured in 5 T as function of current density.

to the value at zero bias, as function of current density J for three microbridges on STO with different thicknesses. The film thickness is indicated for each curve as well as the temperature at which the I - V curve was measured. The variation in ($\frac{dV}{dI}$) with J becomes less strong when the microbridge thickness is increased. Also shown in Fig.3 are similar data of a 10 nm LCMO film grown on an NGO substrate ($T_{MI} = 165$ K) measured at 150 K, again in the steep part of the transition. Although measured in a somewhat smaller current density range we find no nonlinear behavior in films on NGO for thicknesses down to 10 nm.

Besides the well known CMR effect in the transition, we also observe a strong MR effect at low temperatures both for microbridges on STO and on NGO. As becomes clear from Fig.4a this effect too depends on the microbridge thickness. For the 17 nm thick bridge the $R(T)$ curves at 0 T and 5 T almost overlap, but for the 10 nm thick bridge a high magnetic field induces a significant reduction in resistance at low temperature. The magnitude of the low temperature MR increases with reducing film thickness reaching about an order of magnitude for the 6.4 nm thick film, see Fig.4b. Furthermore, also the (unstrained) 10 nm thick film on NGO shows a MR effect, of 50 % at low temperature. Apparently, even for the unstrained LCMO microbridge an applied magnetic field can result in an increased metallicity at low temperature. On the other hand,

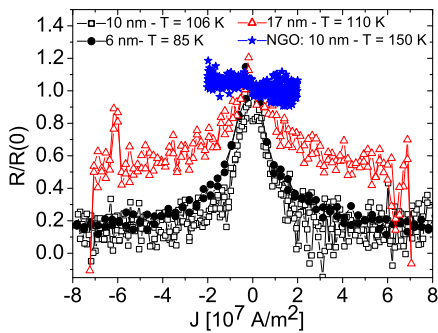


FIG. 3: (color on-line) Numerical derivatives dV/dI of the I - V curves for three different bridges on STO. The curves are normalized w.r.t. the zero bias resistivity. Film thicknesses are indicated as well as the temperature at which the I - V was measured. For all films the curves are shown for the temperature where the largest reduction as function of applied current occurred. The zero bias resistances are, $d = 17$ nm: $R(0) = 0.3$ M Ω , $d = 10$ nm: $R(0) = 4.0$ M Ω and $d = 6$ nm: $R(0) = 4.3$ M Ω . Also shown is the $\frac{dV}{dI}$ curve at $T = 150$ K of the 10 nm LCMO film on NGO which does not show nonlinear behavior.

we stress that in this regime of enhanced MR the I - V characteristics are simply ohmic.

Behavior as found here under the controlled circumstances of substrate, sample thickness, and bridge width, has not been reported before. Nonlinear behavior was observed recently in thick unstructured and strongly oxygen deficient samples [8], but temperature regime, magnetization and field dependence were all different, and it is difficult to connect that work to our observations, in particular since the EELS characterization showed that oxygen deficiency is not an issue in our LCMO films. A concern can be that the observations are an artefact caused by Joule heating in the microbridge. The peak resistivity is around $\rho \sim 10^5$ - 10^6 $\mu\Omega$ cm which we can use to estimate the effect of Joule heating in the measured current density range. The power inserted into the bridge is of the order of μ W; the estimated Joule heating would be in the mK range which is clearly negligible. Furthermore, heating would lead to different nonlinear behavior, namely increasing resistance with increasing current, and can be ruled out as a possible cause for the observed nonlinearities. Another concern could be the influence of the structural phase transition, tetragonal to cubic, which occurs in the STO substrate at $T = 105$ K. Since our LCMO films are epitaxial this could influence microbridge properties. However, we have shown that the observed nonlinear behavior can occur at different temperatures, both above and below $T = 105$ K. This indicates that the nonlinear behavior is not an STO-induced effect but intrinsic to the material LCMO.

We conclude from this that the non-linear behavior

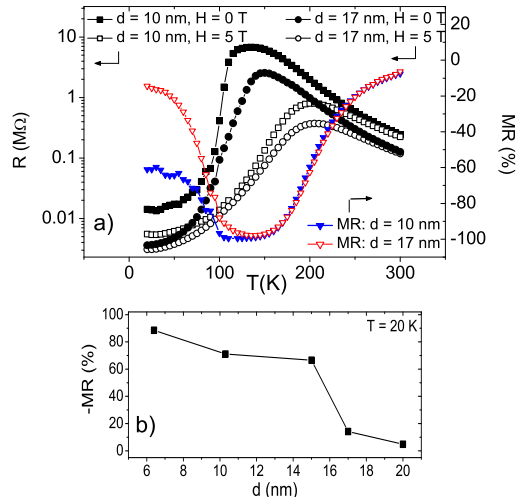


FIG. 4: (color on-line) a) $R(T)$ behavior in 0 T and 5 T of a 17 nm thick and 10 nm thick microbridge. The calculated magnetoresistance as function of temperature is also shown. b) The calculated magnetoresistance ($MR(\%) = \frac{R_{5T} - R_{0T}}{R_{0T}} \times 100\%$) as function of film thickness at $T = 20$ K.

has to be the fingerprint of an organized phenomenon intrinsic to the electron matter formed in the manganite. Next we discuss the different regimes we believe are present, c.q. the different states of the microbridge as it is warmed through the metal-insulator transition. In Fig.5 we provide the $R(T)$ data of the 10 nm microbridge again, in order to help in identifying the various regimes. At low temperature (region I), the strong MR effects show that a high magnetic field can still assist in increasing the metallicity of the microbridge. We believe this to derive from static inhomogeneities which lead to a relatively high residual resistance in the thinnest films and locally frustrate the DE-type metallic state which then forms easier in a (high) magnetic field. The effect is rather similar to the MR reported in Ref.[9] in thin films of $La_{0.8}Ca_{0.2}MnO_3$ which also exists down to the lowest temperatures.

Upon warming into the transition the conduction electrons become more localized, with the Jahn-Teller splitting of the e_g -levels, assisted by the strain in the film, leading to polaron formation. In the steep part of the transition we start to observe strongly nonlinear behavior, and increasing conductance with current. The nonlinearities are fully reversible, indicating that the process which enhances the conductance is not a first-order transition. A scenario in which current transforms a possible antiferromagnetic insulator to a ferromagnetic metal, e.g. through spin torque processes, is not likely, since the closeness of the M-I transition in LCMO to a first-order transition [10] would probably render this process hysteretic. The scenario we propose instead is

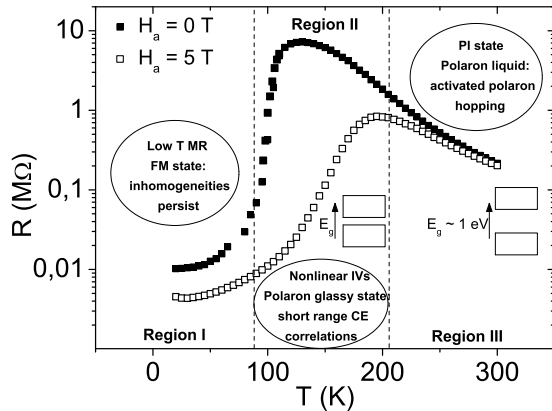


FIG. 5: Proposed scheme for the metal-insulator transition in LCMO ($R(T)$ for the 10 nm microbridge at $J = 2 \times 10^6$ A/m²). Region I: at low temperature the material is in a FM state but nanoscale inhomogeneities persist. Region II: in the transition e_g electrons are localized by Jahn-Teller splitting resulting in the formation of a glassy state of correlated (CE-type, charge ordered) polarons. Region III: at a certain temperature above the transition the polaron correlations break down and the system becomes a polaron liquid with only single dynamic polarons. In the graph the JT-splitting is indicated with $E_g \sim 1$ eV in the polaron liquid state.

that of current-induced melting of an intervening phase which can sustain a voltage difference, while its electrical properties are extraordinarily sensitive to the injection of charge carriers as occurs in the high current state. Such a phase was actually demonstrated to exist, and is called the polaron glass phase [5]. We can understand the origin of this phase by remembering that at higher doping of $x \geq 0.5$, the material is antiferromagnetic and charge and orbital ordered. At lower doping $x = 0.33$ (our material), this ordering is frustrated, but polaron correlations can still occur. In ref.[5] it was shown through neutron scattering experiments that a correlated polaron (glass) phase is formed in LCMO single crystals. The nanoscale structural correlations occur just above T_{MI} . The development of these static (charge ordered, CE-type) polaron structures trap electrons and drive the system into the insulating state. In our case the correlated regions already start to occur below T_{MI} and become more abundant when the bridge is warmed through the transition, a process facilitated by the strain, which causes more disorder on nanoscales as well as larger Jahn-Teller distortions and smaller band-widths. The resulting glass phase fully

closes the bridge off. The injection of carriers into this nascent state by applying a chemical potential difference works against the formation of the polaron correlations and drives the system to a different, more metallic, equilibrium. We note that the large CMR effect in the transition is in itself related to the occurrence of the correlated polaron phase, as reported both experimentally [11, 12] and theoretically [13], while a similar scenario was suggested for the bilayer compound $\text{La}_{1.2}\text{Sr}_{1.8}\text{Mn}_2\text{O}_7$ [14]. Much weaker CMR effects are observed in systems with only single dynamic polarons (large bandwidth materials such as $\text{La}_{0.67}\text{Sr}_{0.33}\text{MnO}_3$). Warming into region III, the polaron correlations break down (polaron liquid) and conduction is governed by thermally activated (single) polaron hopping.

In summary, we find that, upon reducing the size of a strained LCMO film grown on an STO substrate, novel behavior in the transport properties occurs, notably nonlinear current-voltage characteristics. This is not found in wider bridges or when strain is absent (films on NGO). As a possible explanation we use the concept of a phase of glassy polarons which is formed in the M-I transition, assisted by the strain, and which is very sensitive to the injection of charge carriers, leading to current-induced melting of the newly forming insulating state.

We thank I. Komissarov for discussions, and M. Porcu and H. Zandbergen for performing the EELS measurements. This work was part of the research program of the Stichting voor Fundamenteel Onderzoek der Materie (FOM), which is financially supported by NWO.

* E-mail: aarts@physics.leidenuniv.nl

- [1] C. Zener, Phys. Rev. **82**, 403 (1951).
- [2] J. Aarts *et al.*, Appl. Phys. Lett. **72**, 2975 (1998).
- [3] K. Dörr, J. Phys. D: Appl. Phys. **39**, R125 (2006).
- [4] M. Uehara *et al.*, Nature **399**, 560 (1999).
- [5] J.W. Lynn *et al.*, Phys. Rev. B **76**, 014437 (2007); and references therein.
- [6] C. Beekman *et al.*, Phys. Rev. B, in preparation.
- [7] C. Beekman *et al.*, Appl. Phys. Lett. **91**, 062101 (2007).
- [8] S.J. Liu *et al.*, J. Appl. Phys. **103**, 023917 (2008).
- [9] M. Eblen-Zayas *et al.*, Phys. Rev. Lett. **94**, 037204 (2005).
- [10] D. Kim *et al.*, Phys. Rev. Lett. **89**, 227202 (2002).
- [11] V. Kiryukhin *et al.*, Phys. Rev. B, **70**, 214424 (2004).
- [12] V. Moshnyaga *et al.*, Phys. Rev. B **79**, 134413 (2009).
- [13] C. Sen *et al.*, Phys. Rev. Lett. **98**, 127202 (2007).
- [14] N. Mannella *et al.*, Phys. Rev. B **76**, 233102 (2007).